Research Square

Preprints are preliminary reports that have not undergone peer review.
They should not be considered conclusive, used to inform clinical practice,
or referenced by the media as validated information.

Projections of temperature extremes and heatwaves in Goiânia, Brazil: intensity, duration, and persistence under CMIP6 scenarios

Elis Dener Lima Alves

elis.alves@ifgoiano.edu.br

Instituto Federal Goiano

Research Article

Keywords: Climate modeling, seasonal variability, regional climatology, temperature distribution, intermodel uncertainty

Posted Date: November 4th, 2026

DOI: https://doi.org/10.21203/rs.3.rs-11406944/v1

License: This work is licensed under a Creative Commons Attribution 4.0 International License.
Read Full License

Additional Declarations: No competing interests reported.

Abstract

This study assessed changes in maximum air temperature, daytime and nighttime extremes, and heatwaves in Goiânia under SSP1-2.6, SSP2-4.5, SSP3-7.0, and SSP5-8.5 for 2021–2040, 2041–2060, and 2081–2100. Daily NEX-GDDP-CMIP6 series from 31 global climate models were aggregated over the municipality; maximum temperatures were evaluated against ERA5 and INMET observations. Mean daily maximum-temperature changes used the 1995–2014 baseline; extremes used 1985–2014. Heatwaves comprised at least six consecutive days above model- and calendar-day-specific historical P90 thresholds. The multimodel median summarized projections, with performance weighting as a sensitivity analysis. In 2081–2100, median warming ranged from 1.24°C under SSP1-2.6 to 5.15°C under SSP5-8.5, reaching 6.96°C in October under the latter. Median annual heatwave-day increases were 44.60 and 260.60 days, respectively; warm-night frequency increased by 75.69 percentage points under SSP5-8.5. Weighting reduced this scenario's median warming from 5.15 to 4.70°C. Longer heatwaves and greater hot-day persistence indicate substantial changes in Goiânia's temperature-extreme regime, especially under SSP5-8.5.

1. Introduction

Monteiro dos Santos *et al.* (2024) found increasing heatwave frequency in the Goiânia Metropolitan Region during 1970–2020, greater recent variability in event duration, and concentration of events in September–October in central-western Brazilian metropolitan regions. These changes motivate investigation under future emissions pathways.

Heatwave changes involve intensity, occurrence, and continuity. Perkins-Kirkpatrick and Lewis (2020) found regional differences in these trends and a strong association between increasing heatwave days and cumulative heat. In Brazilian projections, longer episodes can merge, reducing event counts despite increasing total days (Ballarin *et al.*, 2024). Frequency, duration, and intensity therefore describe distinct thermal changes.

Using NEX-GDDP-CMIP6, Dantas *et al.* (2025) assessed temperature and precipitation extremes and projected increases in hot days and annual warm-spell days (WSDI) across Brazilian municipalities under SSP2-4.5 and SSP5-8.5. For Belém, Souza *et al.* (2026) assessed heatwave frequency, duration, and intensity under SSP1-2.6, SSP2-4.5, SSP3-7.0, and SSP5-8.5 using CMIP6 models evaluated against local stations and bias-corrected through Quantile Delta Mapping.

NEX-GDDP-CMIP6 provides daily simulations bias-corrected and spatially disaggregated to 0.25° (Thrasher *et al.*, 2022). Maximum and minimum temperatures support analysis of daytime and nighttime extremes and consecutive threshold exceedances. Aggregation over Goiânia provides a common spatial basis for comparing models, scenarios, and indicators.

Model combination also affects projections. Weighting by performance and independence can modify CMIP6 warming estimates and spread (Brunner *et al.*, 2020), but requires application-specific evaluation

and generalization tests (Abramowitz *et al.*, 2019). Here, equal weighting is compared with weighting by performance in representing local temperature characteristics.

This study assesses mean daily maximum-temperature changes and extremes in Goiânia under four SSPs and three future horizons, examining warming seasonality, annual daytime and nighttime extremes, warm-day and warm-night frequencies, heatwave frequency, duration, and intensity, and hot-day persistence.

Maximum-temperature simulations are evaluated against ERA5, with INMET A002 as a complementary reference. The study jointly examines historical temperature characteristics, hot-day persistence, and sensitivity of warming estimates to performance weighting based on 2015–2025.

2. Materials and methods

Figure 1 summarizes data assembly, municipal aggregation of gridded series, GCM evaluation, and projection synthesis. Equal weighting provides the main reference; performance weighting tests sensitivity. Intermodel distributions and sign agreement describe uncertainty.

2.1 Study area

Goiânia, the capital of Goiás in central-western Brazil's Cerrado biome (Fig. 2), was delineated using the IBGE 2025 municipal boundary. Its 729.296 km² contained 1,437,366 inhabitants in the 2022 census, a density of 1,970.90 inhabitants km^{-2} (IBGE, 2025).

At approximately 791 m mean elevation, Goiânia has expanded with population growth (Sousa and Ferreira, 2012). Urbanization has differentiated land surface temperatures among built-up, vegetated, and peripheral areas (Nascimento and Oliveira, 2011; Sousa and Ferreira, 2012).

Goiânia's predominant Köppen–Geiger class is Aw, tropical with a dry winter (Cardoso *et al.*, 2014). Rainfall occurs mainly in October–April, followed by the May–September dry season. Mean annual precipitation is 1,494.66 mm (Casaroli *et al.*, 2018).

2.2 Climate data, scenarios, and analysis periods

NASA Earth Exchange Global Daily Downscaled Projections–CMIP6 (NEX-GDDP-CMIP6) supplies daily fields from Coupled Model Intercomparison Project Phase 6 (CMIP6) simulations on a 0.25° × 0.25° grid using Bias-Correction Spatial Disaggregation (BCSD) (Eyring *et al.*, 2016; Thrasher *et al.*, 2022). One realization per global climate model (GCM) was used.

Daily maximum near-surface air temperature (tasmax) was the main variable; daily minimum temperature (tasmin) supported the relevant extreme indices. Temperatures were converted from kelvin to degrees Celsius. No additional bias correction was applied to the already corrected dataset.

ScenarioMIP pathways SSP1-2.6, SSP2-4.5, SSP3-7.0, and SSP5-8.5 combine socioeconomic pathways and forcing levels, allowing comparison under contrasting development and emissions conditions (O'Neill *et al.*, 2016; Riahi *et al.*, 2017).

Historical evaluation included 31 GCMs. Future availability yielded 29, 30, 25, and 31 GCMs under SSP1-2.6, SSP2-4.5, SSP3-7.0, and SSP5-8.5, respectively. All available combinations meeting processing requirements were retained.

Mean daily maximum-temperature changes used 1995–2014 as the baseline and three 20-year windows: early (2021–2040), middle (2041–2060), and late century (2081–2100). Extreme indices and percentile thresholds used the 30-year baseline 1985–2014.

2.3 Spatial processing and climate model evaluation

Municipal temperatures were area-weighted means of overlapping grid cells. The boundary and cells were transformed to an equal-area coordinate system, and their intersection areas defined fixed cell weights (Eq. 1).

$$w_i = \frac{A_i}{\sum_{j=1}^{n} A_j}$$

1

Here, A_i is the area of intersection between cell i and the municipality, and n is the total number of grid cells with a positive intersection area. For each day t, $V_t \subseteq \{1, \ldots, n\}$ denotes the indices of cells with valid temperature values. The representative daily temperature was calculated as:

$$T_t = \frac{\sum_{i \in V_t} w_i T_{i,t}}{\sum_{i \in V_t} w_i}$$

2

Here, $T_{i,t}$ is the temperature of cell i on day t. The same subset of valid cells was used in the numerator and denominator, thereby renormalizing the weights when values were missing. When all overlapping cells were valid, the denominator equaled one. Days with no valid cells were assigned a missing value. The climate fields were not spatially resampled, intersection-area weights determined each cell's contribution to the municipal mean.

INMET automatic station A002 provided a complementary point reference (INMET, n.d.). Daily maxima were the highest valid hourly air temperatures within each UTC day, without a minimum hourly-coverage requirement. Available 2001–2014 records were evaluated separately from the spatial ERA5 reference.

Evaluation covered climatological mean, median, standard deviation, and interquartile range; monthly-cycle bias, mean absolute error (MAE), root mean square error (RMSE), correlation, annual range, and

peak month; and distribution percentiles P05, P10, P25, P50, P75, P90, P95, and P99.

Historical hot conditions were evaluated using percentages above reference P90 and P95 and mean and maximum run lengths above reference P90. Thresholds pooled daily reference values over 1995–2014 (ERA5) or available 2001–2014 records (INMET), and were applied to both reference and GCM series. They differ from the calendar-day thresholds used for climate extremes. Comparisons emphasize climatological properties because free-running GCMs are not expected to reproduce observed daily weather sequences.

Screening required at least 365 paired valid dates, coverage of ≥ 70% of valid reference dates in the common period, and at least ten calendar months. All 31 GCMs passed against both references and represented all twelve months in period-level summaries. Paired coverage was 98.56–100% against ERA5 and 98.62–100% against INMET; these percentages describe data availability, not daily weather agreement.

Daily paired bias, MAE, RMSE, Pearson correlation, and Deming regression were supplementary diagnostics. GCMs were evaluated through climatology, seasonality, distributions, extremes, and persistence, without ranking by daily correspondence.

The temporally separate 2015–2025 assessment supplied performance metrics for the weighting sensitivity analysis.

2.4 Climate projections and multimodel ensembles

For each GCM, SSP, and horizon, mean daily maximum-temperature change was the future climatology minus that model's 1995–2014 climatology:

$$\Delta T_{m,s,p} = \overline{T}_{m,s,p} - \overline{T}_{m,ref}$$

3

Here, $\Delta T_{m,s,p}$ is the projected change for model m, SSP s, and future period p; $\overline{T}_{m,s,p}$ is the future-period climatology, and $\overline{T}_{m,ref}$ is the model's historical baseline climatology.

The primary ensemble gave equal weight to each available GCM. Its median limits the influence of extreme model values; P05, P25, P75, P95, and the interquartile range (P75 minus P25) summarize spread.

Sign agreement was the percentage of available GCMs sharing the ensemble median's sign:

$$A_{s,p} = \frac{100}{N_{s,p}} \sum_{m \in M_{s,p}} \mathrm{I}\left[\mathrm{sgn}(\Delta T_{m,s,p}) = \mathrm{sgn}(\widetilde{\Delta T}_{s,p})\right]$$

4

Here, $M_{s,p}$ is the set of available models, $N_{s,p} = |M_{s,p}|$, $\widetilde{\Delta T}_{s,p}$ is the ensemble median, and I equals one when the stated condition holds and zero otherwise. Sign agreement was used as a supplementary description of directional consistency across models.

The empirical P05–P95 interval describes available GCM spread conditional on the SSP, not a probabilistic confidence interval or full future-climate uncertainty.

Sensitivity weights were derived separately within each SSP from 2015–2025 performance against ERA5 using five tasmax criteria: absolute difference between period means; monthly climatological-cycle RMSE; MAE across P50, P90, P95, and P99; absolute error in the percentage of days above ERA5 P90; and absolute error in the probability of a hot day following another.

Each criterion was divided by the median of its strictly positive, finite errors across GCMs with available results within the same SSP. Thus, $e_{m,s,j} = \frac{E_{m,s,j}}{a_{s,j}}$, where $E_{m,s,j}$ is the unscaled error and $a_{s,j}$ is the corresponding positive-error median. The multidimensional performance distance was:

$$D_{m,s} = \sqrt{\frac{1}{J}\sum_{j=1}^{J} e_{m,s,j}{}^{2}}$$

5

Here, J = 5, with equal criterion contributions. Every retained GCM–SSP combination had five finite, strictly positive full-period errors, requiring no fallback for missing criteria or undefined normalization scales.

Initial weights followed a decreasing exponential function, normalized over available models within each SSP:

$$w_{m,s}{}^{(0)} = \frac{\exp[-\left(\frac{D_{m,s}}{\widetilde{D}_s}\right)^{2}]}{\sum_{l \in M_s} \exp[-\left(\frac{D_{l,s}}{\widetilde{D}_s}\right)^{2}]}$$

6

Here, $\widetilde{D}_s$ is the median performance distance across the available GCMs in SSP s. Weight stability was assessed using 500 bootstrap replicates with year as the resampling unit and random seed 42. For each model and SSP, the coefficient of variation was the sample standard deviation of its bootstrap weights divided by their mean. CV entered the stability factor as a dimensionless ratio:

$$f_{m,s} = \frac{1}{1 + CV_{m,s}}$$

7

Initial weights were shrunk toward uniform weighting according to temporal stability:

$$u_{m,s} = f_{m,s} w_{m,s}{}^{(0)} + (1 - f_{m,s}) \frac{1}{N_s}$$

8

Weights were capped at three times the uniform weight before final renormalization:

$$c_{m,s} = \min(u_{m,s}, \frac{3}{N_s}), \quad w_{m,s} = \frac{c_{m,s}}{\sum_{l \in M_s} c_{l,s}}$$

9

Here, N_s is the number of GCMs with available performance weights in SSP s. The cap was applied before the final weights were normalized to sum to one. No model reached the cap in the full-period analysis.

For each SSP–period, weights were renormalized over models with valid projections and performance weights. Weighted quantiles sorted changes in ascending order and linearly interpolated against cumulative normalized-weight midpoints:

$$z_i = \sum_{l=1}^{i} v_{(l)} - \frac{v_{(i)}}{2}$$

10

Here, $v_{(i)}$ is the normalized weight associated with the ith ordered projected change. The weighted quantile at probability q was obtained by linear interpolation between the ordered changes and their corresponding z_i values. This estimator was used for the weighted median and P05, P25, P75, and P95.

The equal-weight median remained the main reference; weighting assessed sensitivity of change magnitudes, without assigning probabilities to GCMs or SSPs. The weighting period overlaps 2021–2025, or 25% of the first projection window, so this comparison does not independently validate 2021–2040.

2.5 Temperature extremes and heatwaves

Extreme indices were calculated annually from tasmax and tasmin for each GCM before ensemble synthesis, using model-specific 1985–2014 thresholds.

Following ETCCDI (Zhang *et al.*, 2011), with the percentile adjustment below, TXx and TNx are annual maxima of daily maximum and minimum temperature. TX90p and TN90p are annual percentages above

corresponding calendar-day P90 thresholds. WSDI counts annual days in runs of ≥ 6 consecutive days with tasmax above calendar-day P90.

Each GCM's calendar-day P90 used a centered five-day window and the median-unbiased Hyndman–Fan type 8 quantile estimator (Hyndman and Fan, 1996).

Baseline TX90p and TN90p used leave-one-year-out (LOO) thresholds, estimated excluding the evaluated year and then applied to it. This reduces self-inclusion but differs from Climdex's replacement bootstrap and need not reproduce its results.

Heatwaves used the WSDI criterion. Annual metrics were event count (HW_events), total days (HW_total_days), maximum duration (HW_max_duration), and mean duration (HW_mean_duration), calculated as total days divided by count. HW_total_days therefore equals WSDI.

Daily intensity was tasmax minus its P90 threshold (°C), summarized annually as HW_mean_intensity and HW_peak_intensity.

In years with temperature data but no heatwaves, annual counts, total days, durations, and intensities were zero and retained in period means. Zeros indicate event absence rather than physical intensity of a nonexistent event.

HW_persistence is the conditional probability that a day above P90 follows another, including hot days outside qualifying events. For eligible consecutive-day pairs within year y:

$$P_y = \frac{\sum_{t \in J_y} H_t H_{t+1}}{\sum_{t \in J_y} H_t}$$

11

Here, H_t equals one when tasmax on day t exceeds its calendar-day P90 and zero otherwise. J_y denotes transitions for which t and t + 1 are consecutive days in the same native-calendar year and both temperatures and thresholds are valid. The final day of a year has no eligible successor within that year. Persistence is undefined when the denominator is zero. In the annual results, the five years with no days above P90 had missing persistence values; years without six-day heatwaves could nevertheless have positive hot-day persistence.

Runs and transitions were calculated within each year, potentially splitting cross-year episodes. Period summaries were arithmetic means of annual indices, omitting undefined persistence. Changes were future minus baseline means: TX90p and TN90p in percentage points and HW_persistence in probability units (×100 for percentage points).

Table I. Temperature-extreme indices and heatwave metrics used in this study.

Index	Definition used	Unit
TXx	Annual maximum of tasmax	°C
TNx	Annual maximum of tasmin	°C
TX90p	Days with tasmax > calendar-day P90	%
TN90p	Days with tasmin > calendar-day P90	%
WSDI	Days in sequences of ≥ 6 days with tasmax > P90	days
HW_events	Number of heatwaves	events
HW_total_days	Total heatwave days	days
HW_max_duration	Annual maximum event duration	days
HW_mean_duration	Mean event duration	days
HW_mean_intensity	Mean tasmax exceedance above P90 during events	°C
HW_peak_intensity	Maximum tasmax exceedance above P90	°C
HW_persistence	Probability $P(H_{+1} \mid H)$	Proportion

For 2021–2040, 2041–2060, and 2081–2100, model-specific changes relative to 1985–2014 were summarized by the median, P05, P25, P75, P95, and sign agreement. Thresholds were relative to each GCM's climatology, with no absolute maximum-temperature cutoff.

3. Results and discussion

3.1 Representation of the historical climate

All 31 GCMs overestimated mean daily maximum temperature and P90, P95, and P99 against both references. Median mean biases were 1.89°C (model range 1.63–2.25°C) against ERA5 in 1995–2014 and 1.07°C (0.77–1.50°C) against INMET A002 in available 2001–2014 records (Table II). These results characterize the bias-corrected, downscaled NEX-GDDP-CMIP6 series.

The references differ in period and spatial support: INMET measures a point, whereas ERA5 is aggregated over the municipality. Larger differences against ERA5 cannot alone be attributed to urbanization or a particular reanalysis error (Hersbach *et al.*, 2020).

Both references and all 31 GCMs peak in September (Fig. 3a–b). Median monthly-cycle correlations were 0.94 against ERA5 and 0.84 against INMET; RMSEs were 1.94 and 1.33°C. ERA5 median monthly biases approached 2.50°C in May–July. INMET biases peaked in May–August (1.87–2.01°C), becoming negative in December (− 0.24°C; Fig. 3c–d). Correct peak timing thus coexists with magnitude and seasonal bias.

Median bias increased toward the distribution tail: ERA5 values were 1.55, 2.56, and 3.61°C at P50, P95, and P99, versus 0.67, 2.19, and 3.05°C for INMET. This nonuniform shift is incompletely described by mean or seasonal-cycle diagnostics. Median simulated exceedances were 27.30% above ERA5 P90 and 21.42% above INMET P90, versus approximately 10% in the references. Median mean run lengths were 5.25 and 4.95 days, compared with reference values of 3.62 and 2.92 days. These more frequent, longer spells partly reflect the positive distribution shift and cannot be attributed solely to temporal dependence. Common reference thresholds also differ from the model- and calendar-day-specific thresholds used for projections.

NEX-GDDP-CMIP6 correction uses the Global Meteorological Forcing Dataset, so agreement with other references is not assured and application-specific evaluation remains necessary (Thrasher *et al.*, 2022). The identified biases affect absolute temperatures and threshold exceedances in Goiânia. Model-relative anomalies express warming against each model's climatology but do not remove limitations in future responses or extreme distributions. The 2015–2025 assessment extends this diagnosis.

Table II. Historical performance of the 31 GCMs in representing maximum temperature in Goiânia.

Metric	ERA5 (1995–2014)	INMET (2001–2014)
Mean bias (°C)	1.89 (1.63–2.25)	1.07 (0.77–1.50)
Monthly-cycle RMSE (°C)	1.94 (1.72–2.29)	1.33 (1.06–1.70)
Monthly-cycle correlation	0.94 (0.90–0.97)	0.84 (0.75–0.91)
P95 bias (°C)	2.56 (2.13–3.27)	2.19 (1.46–2.99)
P99 bias (°C)	3.61 (2.98–4.75)	3.05 (2.05–4.22)
Days above reference P90 (%)	27.30 (23.16–31.33)	21.42 (16.82–26.65)
Mean run duration above reference P90 (days)	5.25 (4.21–6.41)	4.95 (4.04–6.22)

Note: Bias is GCM minus reference. Correlation uses the 12 monthly climatological values. P90 thresholds in this evaluation were derived from all daily values of each reference. Statistics were calculated separately for each model before intermodel synthesis.

3.2 Model performance during the separate 2015–2025 period

The 2015–2025 ERA5 evaluation included 115 model–scenario combinations: 29, 30, 25, and 31 GCMs under SSP1-2.6, SSP2-4.5, SSP3-7.0, and SSP5-8.5. Ensemble sizes reflect availability, without performance exclusion. Median absolute mean errors were 2.13–2.28°C, monthly-cycle RMSEs 2.24–2.41°C, and MAEs across P50, P90, P95, and P99 2.38–2.52°C (Table III). Persistent discrepancies do not establish deterioration because periods differ in duration, climatic conditions, and partly model composition.

Median absolute errors were 15.30–17.02 percentage points for ERA5 P90 exceedance frequency and 0.086–0.097 for hot-day persistence. These quantify discrepancy magnitudes, without identifying direction, beyond mean-temperature diagnostics.

Scenario medians differed less than their overlapping interquartile ranges for all five criteria (Table III), showing no clear descriptive performance separation. Partly differing model sets also preclude ranking pathway plausibility.

Errors varied annually (Fig. 4a–e). Across scenarios, median quantile errors ranged from 0.96–1.54°C in 2015 to 3.21–3.54°C in 2022; persistence errors were 0.033–0.039 in 2021 and 0.202–0.224 in 2018. Evaluation depends on sampled years and internal variability in simulations and references, without assumed daily correspondence. Internal variability must be distinguished from model-response differences (Brunner *et al.*, 2020).

Across 500 annual resamples, median weight coefficients of variation were 23.5–24.4%, with some model–scenario values reaching 85.0% under SSP5-8.5 (Fig. 4f). Shrinkage toward uniform weights reduces the influence of temporally unstable performance differences without establishing predictive skill.

Because 2015–2025 supplies the weights, it does not independently test weighted-ensemble superiority. Application-appropriate out-of-sample testing is required (Abramowitz *et al.*, 2019). Weighting therefore remains a sensitivity analysis (Section 3.5).

Table III. Climate model performance against ERA5 during 2015–2025.

Metric	SSP1-2.6	SSP2-4.5	SSP3-7.0	SSP5-8.5
Number of GCMs	29	30	25	31
Absolute mean error (°C)	2.13 (2.05–2.31)	2.21 (1.99–2.42)	2.28 (2.02–2.47)	2.17 (1.97–2.31)
Monthly-cycle RMSE (°C)	2.24 (2.12–2.49)	2.30 (2.12–2.52)	2.41 (2.18–2.53)	2.31 (2.08–2.43)
Mean absolute quantile error (°C)	2.41 (2.11–2.72)	2.48 (2.13–2.81)	2.52 (2.30–2.97)	2.38 (2.17–2.87)
Absolute hot-day frequency error (pp)	15.62 (13.81–18.82)	15.30 (13.89–18.47)	17.02 (14.65–19.63)	15.37 (13.95–17.67)
Absolute persistence error	0.087 (0.065–0.101)	0.086 (0.065–0.106)	0.092 (0.057–0.106)	0.097 (0.062–0.118)

Note: Metrics were calculated over the full 2015–2025 period before intermodel synthesis. Quantile error considers P50, P90, P95, and P99. Persistence error is the absolute difference between conditional probabilities and is dimensionless.

3.3 Projected maximum-temperature changes across scenarios and time horizons

All available models project increases in municipal mean daily maximum temperature across scenarios and horizons relative to 1995–2014, with differing magnitudes and spread, especially late in the century (Table IV; Fig. 5). This variable differs from absolute or annual maximum temperature.

Table IV. Projected changes in mean daily maximum temperature in Goiânia relative to 1995–2014.

Scenario	Models	2021–2040	2041–2060	2081–2100
SSP1-2.6	29	0.76 (0.42–1.46)	1.31 (0.85–2.24)	1.24 (0.45–2.58)
SSP2-4.5	30	0.91 (0.54–1.93)	1.65 (1.10–2.72)	2.56 (1.81–4.29)
SSP3-7.0	25	0.92 (0.56–1.81)	1.73 (1.25–2.90)	3.79 (2.94–6.22)
SSP5-8.5	31	1.09 (0.58–1.98)	2.17 (1.40–3.77)	5.15 (3.58–8.32)

Note: Values are in °C, expressed as medians with P05–P95 in parentheses, based on changes calculated separately for each model. The reference ensemble assigns equal model weights. Percentiles describe intermodel spread, not confidence intervals.

In 2021–2040, medians range from 0.76°C under SSP1-2.6 to 1.09°C under SSP5-8.5, with extensively overlapping scenario intervals. Separation grows in 2041–2060 (1.31–2.17°C). By 2081–2100, medians

reach 1.24, 2.56, 3.79, and 5.15°C under SSP1-2.6, SSP2-4.5, SSP3-7.0, and SSP5-8.5, respectively.

SSP1-2.6 changes little from 1.31°C in 2041–2060 to 1.24°C in 2081–2100, suggesting stabilization rather than demonstrating significant cooling. Almazroui *et al.* (2021) likewise found little additional SSP1-2.6 warming but increases exceeding 5°C in tropical South America under SSP5-8.5. Their shared 1995–2014 baseline permits contextual comparison, but their 1° mean air temperature for 2040–2059 and 2080–2099 differs from municipal daily maxima, precluding direct equivalence.

Ortega *et al.* (2021) found warming agreement among CMIP5/CMIP6 models for Central and South America, including the Cerrado. Goiânia shares that sign across spatial scales, although shared CMIP6 models limit comparison independence.

Paired contrasts for the 29 models common to SSP1-2.6 and SSP5-8.5 separate scenario from composition effects. Median additional SSP5-8.5 warming was 0.24°C in 2021–2040 (P05–P95: − 0.10 to 0.64°C; 86.2% positive agreement), 0.92°C in 2041–2060, and 3.72°C in 2081–2100 (2.90–5.76°C). All common models showed larger SSP5-8.5 warming in the latter two periods. These medians of paired differences differ from differences between Table IV medians.

Late-century P05–P95 spans 3.58–8.32°C under SSP5-8.5 versus 0.45–2.58°C under SSP1-2.6. Sign agreement thus coexists with magnitude uncertainty. Shared model components and parameterizations limit independence (Abramowitz *et al.*, 2019); quantiles and 100% agreement describe the ensemble, not outcome probabilities.

3.4 Seasonality of projected maximum-temperature changes

Warming peaks during the dry-to-rainy-season transition, with stronger seasonal contrasts under higher forcing (Fig. 6). All monthly medians are positive. October peaks in 11 of 12 combinations; November peaks under SSP1-2.6 in 2081–2100.

In 2021–2040, October medians range from 1.19°C under SSP1-2.6 to 1.59°C under SSP2-4.5, without uniform forcing-level ordering and with overlapping distributions. In 2041–2060, October peaks at 1.93, 2.50, 2.47, and 3.25°C under SSP1-2.6, SSP2-4.5, SSP3-7.0, and SSP5-8.5, respectively.

Late-century seasonal differences widen under SSP3-7.0 and SSP5-8.5 (Table V). Under SSP5-8.5, February warming of 4.14°C contrasts with October's 6.96°C (2.82°C difference). September and November reach 5.91 and 6.28°C, extending strong warming across the transition.

Table V. Lowest and highest monthly median warming in Goiânia during 2081–2100 relative to 1995–2014.

Scenario	Lowest warming	Highest warming	Difference between medians
SSP1-2.6	February: 0.91°C	November: 1.77°C	0.86°C
SSP2-4.5	February: 2.12°C	October: 3.51°C	1.38°C
SSP3-7.0	March: 3.14°C	October: 5.37°C	2.24°C
SSP5-8.5	February: 4.14°C	October: 6.96°C	2.82°C
Note: Differences were calculated before rounding and represent the contrast between the highest and lowest warming in the cycle of monthly medians.			

For Cerrado July–October temperatures, Hofmann *et al.* (2021) estimated the largest historical maximum-temperature increase in October (4.0°C during 1961–2019). The seasonal agreement is contextual: their biome-wide historical changes differ from municipal projections relative to 1995–2014.

Cattelan *et al.* (2024) projected stronger Cerrado precipitation seasonality and vapor pressure deficit, especially during the dry-to-rainy transition. This timing matches Goiânia's warming maximum, but maximum-temperature projections alone cannot establish local rainfall reductions, delayed rains, or increasing vapor pressure deficit.

Goiânia's seasonal pattern also accords with the widening warm–cool month contrast projected for South America under stronger late-century forcing (Almazroui *et al.*, 2021), while differing in variable: municipal daily maxima versus mean air temperature.

October SSP5-8.5 warming in 2081–2100 has P05–P95 of 4.48–10.88°C around 6.96°C. Annual positive unanimity does not cover every monthly combination: some early-century models show small monthly decreases and intervals include zero. All models warm every month under SSP2-4.5, SSP3-7.0, and SSP5-8.5 in 2041–2060 and 2081–2100.

3.5 Sensitivity to model weighting

Performance weighting reduced annual medians in all 12 combinations (differences: − 0.02 to − 0.45°C), preserving positive changes and scenario ordering (Table VI; Fig. 7).

Table VI. Median maximum-temperature warming in Goiânia for the equal-weight and weighted ensembles.

Scenario	Period	Equal weights (°C)	Weighted (°C)	Difference (°C)
SSP1-2.6	2021–2040	0.76	0.73	−0.02
SSP1-2.6	2041–2060	1.31	1.24	−0.07
SSP1-2.6	2081–2100	1.24	1.15	−0.09
SSP2-4.5	2021–2040	0.91	0.85	−0.06
SSP2-4.5	2041–2060	1.65	1.56	−0.09
SSP2-4.5	2081–2100	2.56	2.41	−0.15
SSP3-7.0	2021–2040	0.92	0.89	−0.03
SSP3-7.0	2041–2060	1.73	1.71	−0.02
SSP3-7.0	2081–2100	3.79	3.68	−0.11
SSP5-8.5	2021–2040	1.09	1.03	−0.06
SSP5-8.5	2041–2060	2.17	2.03	−0.14
SSP5-8.5	2081–2100	5.15	4.70	−0.45

Note: Baseline: 1995–2014. Difference = weighted median minus equal-weight median, calculated before rounding.

The largest reduction was late-century SSP5-8.5, from 5.15 to 4.70°C (approximately 8.7%). Reductions were 0.09, 0.15, and 0.11°C under SSP1-2.6, SSP2-4.5, and SSP3-7.0. With no performance exclusions, these shifts reflect changed relative model contributions.

ClimWIP reduced global SSP5-8.5 warming from 4.1 to 3.7°C for 2081–2100 relative to 1995–2014 (Brunner *et al.*, 2020). Both analyses lower central estimates, but ClimWIP combines performance and independence, whereas this study uses local performance and temporal stability; global mean warming also differs from median municipal maximum-temperature change.

Spread did not systematically narrow. Late-century SSP5-8.5 P05–P95 changed from 3.58–8.32 to 3.50–8.30°C, widening from 4.74 to 4.80°C; early-century SSP3-7.0 width fell from 1.25 to 1.03°C. Lower medians therefore do not imply reduced spread.

Effective ensemble sizes based on weight concentration were 26.88, 27.54, 23.31, and 28.36, versus 29, 30, 25, and 31 available models under the four SSPs, indicating limited weight concentration. These are not structurally independent model counts: performance weighting does not correct shared-component dependence (Abramowitz *et al.*, 2019).

Monthly weighted-minus-reference medians ranged from − 0.90 to + 0.03°C. The largest reduction was May under late-century SSP5-8.5 (5.34 to 4.45°C). October still peaked in that combination (6.96 to 6.51°C); across combinations, peaks remained in September–November, although individual peak

months sometimes changed. Transition-season concentration was more stable than the exact peak month.

In out-of-sample tests using future pseudo-observations, O'Reilly *et al.* (2024) found improvements in constrained European regional temperature projections, especially in summer. Here, weighting demonstrates methodological sensitivity without establishing greater future accuracy, so equal weighting remains the primary reference.

3.6 Changes in daytime and nighttime temperature extremes

Daytime and nighttime extremes intensify, and warm days and nights become more frequent relative to 1985–2014 (Table VII; Fig. 8). Indices retain the definitions in Section 2.5.

Late-century TXx median increases are 1.62, 3.03, 4.36, and 5.94°C under the four SSPs; TNx increases are 1.39, 2.64, 4.33, and 5.60°C. Stronger Brazilian warm extremes were also projected using 20 models under RCP4.5/RCP8.5 (Avila-Diaz *et al.*, 2020), although models, scenarios, and baselines differ.

Table VII. Median changes in temperature-extreme indices in Goiânia relative to 1985–2014.

Scenario	Period	ΔTXx (°C)	ΔTNx (°C)	ΔTX90p (pp)	ΔTN90p (pp)
SSP1-2.6	2021–2040	0.73	0.88	9.40	19.14
SSP1-2.6	2041–2060	1.49	1.44	17.13	28.88
SSP1-2.6	2081–2100	1.62	1.39	16.22	28.01
SSP2-4.5	2021–2040	0.92	0.89	11.02	21.26
SSP2-4.5	2041–2060	1.54	1.78	20.98	34.85
SSP2-4.5	2081–2100	3.03	2.64	36.95	50.70
SSP3-7.0	2021–2040	0.92	1.00	11.68	23.45
SSP3-7.0	2041–2060	1.96	1.98	25.32	39.09
SSP3-7.0	2081–2100	4.36	4.33	55.43	65.75
SSP5-8.5	2021–2040	1.58	1.23	14.48	23.94
SSP5-8.5	2041–2060	2.54	2.27	30.74	47.12
SSP5-8.5	2081–2100	5.94	5.60	69.89	75.69
Note: Values are medians of model-specific changes. pp: percentage points.					

TN90p increases exceed TX90p increases in all 12 combinations. Under SSP5-8.5, TX90p/TN90p changes rise from 14.48/23.94 percentage points in 2021–2040 to 69.89/75.69 in 2081–2100. Every

model projects positive changes in both indices across all combinations.

Goiânia follows the increasing hot-day pattern projected across Brazilian municipalities, with stronger high-emission changes extending toward central-western Brazil in later horizons (Dantas *et al.*, 2025). Shared NEX-GDDP-CMIP6 data preclude independent validation; model selection, baselines, and indicators also differ.

Greater TN90p increases do not establish stronger nighttime warming in degrees Celsius: percentile frequencies depend on baseline distributions and thresholds, whereas TXx/TNx describe annual highest values. Late-century TXx changes exceed TNx in all scenarios, with similar values under SSP3-7.0.

De Lima *et al.* (2026) projected declining diurnal ranges across much of South America with stronger minimum-temperature warming and regional contrasts. Such changes require daily maximum-minus-minimum analysis and cannot be inferred from the present annual extremes or frequencies.

SSP1-2.6 TX90p/TN90p changes are similar between middle and late century, suggesting stabilization above historical frequencies; other scenarios continue increasing. Late-century SSP5-8.5 P05–P95 is 3.82–9.37°C for TXx and 4.16–8.13°C for TNx. Early-century TXx intervals cross zero in all scenarios despite approximately 90–93% positive agreement.

3.7 Heatwave frequency, duration, intensity, and hot-day persistence

Heatwave counts, days, durations, and intensities have positive median changes, with stronger late-century scenario separation (Table VIII; Fig. 9). Under the six-day, model- and calendar-day-specific 1985–2014 P90 criterion, total annual heatwave days equal WSDI.

Median additional heatwave days range from 21.25 days yr^{-1} under SSP1-2.6 to 33.22 under SSP5-8.5 in 2021–2040. By 2081–2100 they reach 44.60, 112.13, 189.07, and 260.60 days yr^{-1} under the four SSPs, with unanimous model agreement on increases.

Using 12-km regional simulations, Ramarao *et al.* (2024) also projected more frequent, longer, and more intense Central and South American heatwaves under RCP2.6, strengthening under RCP8.5. Definitions, periods, and modeling differences preclude direct magnitude comparisons.

Table VIII. Median changes in heatwave indicators in Goiânia for 2081–2100 relative to 1985–2014.

Metric - projected change	SSP1-2.6	SSP2-4.5	SSP3-7.0	SSP5-8.5
Event count (events yr⁻¹)	4.23	8.16	9.78	9.51
Heatwave days - WSDI (days yr⁻¹)	44.60	112.13	189.07	260.60
Annual maximum duration (days)	9.85	22.33	38.67	69.73
Annual mean event duration (days)	4.18	6.80	11.75	19.95
Annual mean intensity (°C)	0.76	1.10	1.68	2.41
Annual peak intensity (°C)	2.61	4.16	5.68	7.23
Hot-day persistence (pp)	14.76	22.67	30.60	35.16
Note: Medians of differences between model-specific period means of annual indicators. Duration and intensity metrics include zeros in years without events.				

Under SSP5-8.5, median annual maximum-duration changes rise from 7.85 days in 2021–2040 to 17.97 in 2041–2060 and 69.73 in 2081–2100. These changes concern period means of annual longest events, not the longest event across a period. Late-century P05–P95 spans 32.34–196.15 days, and mean event duration increases by a median 19.95 days.

Late-century event counts increase by 9.78 yr⁻¹ under SSP3-7.0 versus 9.51 under SSP5-8.5, despite greater total-day increases under the latter. Counts thus incompletely describe intensification. Longer Brazilian heatwaves can merge, reducing counts while adding days (Ballarin *et al.*, 2024); Goiânia's scenario medians are compatible with, but do not demonstrate, this mechanism.

Mean and peak intensities have positive median changes in all scenarios. Late-century increases are 0.76/2.61°C under SSP1-2.6 and 2.41/7.23°C under SSP5-8.5, expressed above historical thresholds rather than as absolute temperatures. Zero-valued event-free years make period means sensitive to both event characteristics and occurrence.

Historically, cumulative heat increases were strongly associated with more heatwave days, while mean intensity responded less uniformly (Perkins-Kirkpatrick and Lewis, 2020), supporting separate assessment of these characteristics.

Hot-day persistence increases in every model, scenario, and horizon, with late-century median increases of 14.76 percentage points under SSP1-2.6 and 35.16 under SSP5-8.5. Including hot days outside six-day events, it reflects greater consecutive-day probability but also increasing exceedance frequency.

Additional heatwave days change little under SSP1-2.6 between middle and late century (43.18 to 44.60 days yr⁻¹), versus 88.97 to 260.60 under SSP5-8.5. These contrasts describe thermal exceptions relative to fixed 1985–2014 thresholds, without accounting for future adaptation or heat tolerance.

3.8 Implications for Goiânia and projection limitations

Contrasting warming, warm-day and warm-night frequencies, and heatwave durations demonstrate the influence of emissions pathways on Goiânia's climate. Persistent changes under SSP1-2.6 also support adaptation.

Goiânia has heterogeneous land surface temperatures (Nascimento and Oliveira, 2011), whereas these projections aggregate air temperature over the municipality. The different variables cannot establish future urban heat island intensification, which requires evolving urban–rural comparisons.

Historical heatwave increases and demographic and racial inequalities in related mortality across 14 Brazilian metropolitan regions, including increasing frequency in Goiânia (Monteiro dos Santos *et al.*, 2024), underscore exposure and social vulnerability in adaptation planning.

Strongest warming during the seasonal transition coincides with historical September–October heatwave concentration in central-western metropolitan regions (Monteiro dos Santos *et al.*, 2024), supporting monitoring then. The greatest monthly mean warming need not coincide with maximum future heatwave frequency.

Adaptation options include tree planting, shared-space shading, and improved building thermal conditions. Requia *et al.* (2025) found associations consistent with protective effects of several greenness indicators on hospital admissions in Brazil, varying by outcome, age, and sex. Goiânia priorities could integrate tree cover, air temperature, housing, population, and service access; municipal projections do not estimate intervention effectiveness.

Daily 0.25° statistically downscaled, bias-corrected projections (Thrasher *et al.*, 2022) do not resolve neighborhoods, streets, or buildings. Municipal-series extremes are not maxima anywhere within the city. Intraurban applications require distributed observations and modeling appropriate to local processes.

Intermodel quantiles and agreement are not probabilities or independent evidence counts, given shared model structures (Abramowitz *et al.*, 2019). One realization per GCM limits internal-variability sampling, and unequal scenario availability complicates small median contrasts.

Lower weighted medians do not establish greater accuracy: 2015–2025 supplies the weights rather than independent validation. Predictive gains require further out-of-sample testing (Abramowitz *et al.*, 2019).

Fixed historical thresholds exclude future physiological or behavioral adaptation. The six-day criterion excludes shorter episodes; annual calculations can split cross-year events; and event-free zeros affect duration and intensity means. Comparisons must account for these choices. The criterion was not calibrated for health alerts.

4. Conclusions

Goiânia projections indicate warming and intensifying daytime and nighttime extremes, warm-day and warm-night frequencies, and heatwave durations, depending on scenario and horizon.

By 2081–2100, median mean daily maximum-temperature changes range from 1.24°C under SSP1-2.6 to 5.15°C under SSP5-8.5 relative to 1995–2014. Scenario separation widens late in the century; October has the greatest warming in most combinations.

Warm-night frequency increases more than warm-day frequency in every combination, without establishing stronger nighttime warming in degrees Celsius. Increasing heatwave days and durations make counts alone insufficient: late-century median additional days reach 44.60 under SSP1-2.6 and 260.60 under SSP5-8.5 relative to 1985–2014.

Weighting lowers warming medians without changing sign or scenario contrast or demonstrating greater accuracy. Central estimates require accompanying intermodel spread. Scenario contrasts support mitigation, while persistent SSP1-2.6 changes support adaptation through monitoring, intervention evaluation, and identification of vulnerable places and groups.

Declarations

Author Contribution

Elis Dener Lima Alves: Conceptualization; Methodology; Software; Validation; Formal analysis; Investigation; Resources; Data curation; Writing – original draft; Writing – review & editing; Visualization; Project administration.

References

1. Abramowitz G, Herger N, Gutmann E, Hammerling D, Knutti R, Leduc M, Lorenz R, Pincus R, Schmidt GA. 2019. ESD Reviews: Model dependence in multi-model climate ensembles: weighting, sub-selection and out-of-sample testing. Earth System Dynamics 10: 91–105. https://doi.org/10.5194/esd-10-91-2019
2. Almazroui M, Ashfaq M, Islam MN, Rashid IU, Kamil S, Abid MA, O'Brien E, Ismail M, Reboita MS, Sörensson AA, Arias PA, Alves LM, Tippett MK, Saeed S, Haarsma R, Doblas-Reyes FJ, Saeed F, Kucharski F, Nadeem I, Silva-Vidal Y, Rivera JA, Ehsan MA, Martínez-Castro D, Muñoz ÁG, Ali MA, Coppola E, Sylla MB. 2021. Assessment of CMIP6 performance and projected temperature and precipitation changes over South America. Earth Systems and Environment 5: 155–183. https://doi.org/10.1007/s41748-021-00233-6
3. Avila-Diaz A, Benezoli V, Justino F, Torres R, Wilson A. 2020. Assessing current and future trends of climate extremes across Brazil based on reanalyses and earth system model projections. Climate Dynamics 55: 1403–1426. https://doi.org/10.1007/s00382-020-05333-z
4. Ballarin AS, Oliveira PTS, Uchôa JGSM, Lima CHR, Zaerpour M, Godoy MRV, Meira Neto AA, Papalexiou SM, Wendland E. 2024. Escalating threat of human-perceived heatwaves in Brazil. Environmental Research Communications 6: 111004. https://doi.org/10.1088/2515-7620/ad9140

5. Brunner L, Pendergrass AG, Lehner F, Merrifield AL, Lorenz R, Knutti R. 2020. Reduced global warming from CMIP6 projections when weighting models by performance and independence. Earth System Dynamics 11: 995–1012. https://doi.org/10.5194/esd-11-995-2020
6. Cardoso MRD, Marcuzzo FFN, Barros JR. 2014. Classificação climática de Köppen-Geiger para o estado de Goiás e o Distrito Federal. Acta Geográfica 8: 40–55. https://doi.org/10.18227/2177-4307.acta.v8i16.1384
7. Casaroli D, Rodrigues TR, Martins APB, Evangelista AWP, Alves Júnior J. 2018. Padrões de chuva e de evapotranspiração em Goiânia, GO. Revista Brasileira de Meteorologia 33: 247–256. https://doi.org/10.1590/0102-7786332004
8. Cattelan LG, Mattos CRC, Pamplona MB, Hirota M. 2024. Mapping climatic regions of the Cerrado: general patterns and future change. International Journal of Climatology 44: 5857–5872. https://doi.org/10.1002/joc.8670
9. Dantas LG, Ferreira AJF, Pinto Junior JA, Cortes TR, Neves DJD, de Oliveira BFA, da Silveira IH. 2025. Projections of extreme weather events according to climate change scenarios and populations at-risk in Brazil. Climatic Change 178: 152. https://doi.org/10.1007/s10584-025-03989-2
10. de Lima DMC, Gomes HB, Ray P, Watanabe M, da Silva MCL, Torres RR, Silva MT, Lyra MJA, Da Silva Bezerra KF. 2026. Projected (2015–2100) nighttime-enhanced warming and regional contrasts in diurnal temperature range across South America: sub-regional assessments from CMIP6. Earth Systems and Environment 10: 11911–11931. https://doi.org/10.1007/s41748-026-01214-3
11. Eyring V, Bony S, Meehl GA, Senior CA, Stevens B, Stouffer RJ, Taylor KE. 2016. Overview of the Coupled Model Intercomparison Project Phase 6 (CMIP6) experimental design and organization. Geoscientific Model Development 9: 1937–1958. https://doi.org/10.5194/gmd-9-1937-2016
12. Hersbach H, Bell B, Berrisford P, Hirahara S, Horányi A, Muñoz-Sabater J, Nicolas J, Peubey C, Radu R, Schepers D, Simmons A, Soci C, Abdalla S, Abellan X, Balsamo G, Bechtold P, Biavati G, Bidlot J, Bonavita M, De Chiara G, Dahlgren P, Dee D, Diamantakis M, Dragani R, Flemming J, Forbes R, Fuentes M, Geer A, Haimberger L, Healy S, Hogan RJ, Hólm E, Janisková M, Keeley S, Laloyaux P, Lopez P, Lupu C, Radnoti G, de Rosnay P, Rozum I, Vamborg F, Villaume S, Thépaut JN. 2020. The ERA5 global reanalysis. Quarterly Journal of the Royal Meteorological Society 146: 1999–2049. https://doi.org/10.1002/qj.3803
13. Hofmann GS, Cardoso MF, Alves RJV, Weber EJ, Barbosa AA, de Toledo PM, Pontual FB, Salles LO, Hasenack H, Cordeiro JLP, Aquino FE, de Oliveira LFB. 2021. The Brazilian Cerrado is becoming hotter and drier. Global Change Biology 27: 4060–4073. https://doi.org/10.1111/gcb.15712
14. Hyndman RJ, Fan Y. 1996. Sample quantiles in statistical packages. The American Statistician 50: 361–365. https://doi.org/10.1080/00031305.1996.10473566
15. IBGE (Instituto Brasileiro de Geografia e Estatística). 2025. Goiânia: Cidades e Estados. Rio de Janeiro: IBGE. Available at https://www.ibge.gov.br/cidades-e-estados/go/goiania.html (accessed on October 9, 2026).

16. INMET (Instituto Nacional de Meteorologia). n.d. Dados históricos anuais: estações meteorológicas automáticas. Brasília: INMET. Available at https://portal.inmet.gov.br/dadoshistoricos/ (accessed on October 9, 2026).
17. Monteiro dos Santos D, Libonati R, Garcia BN, Geirinhas JL, Salvi BB, Lima e Silva E, Rodrigues JA, Peres LF, Russo A, Gracie R, Gurgel H, Trigo RM. 2024. Twenty-first-century demographic and social inequalities of heat-related deaths in Brazilian urban areas. PLOS ONE 19: e0295766. https://doi.org/10.1371/journal.pone.0295766
18. NASA Earth Exchange. 2025. Global Daily Downscaled Projections version 2 (NEX-GDDP-CMIP6 v2.0): Technical note. Updated May 31, 2025. Available at https://www.wdc-climate.de/ui/cerarest/addinfoDownload/NEX_TechNote/NEX-GDDP-CMIP6-v2-Tech_Note.pdf (accessed on October 9, 2026).
19. Nascimento DTF, Oliveira IJ. 2011. Análise da evolução do fenômeno de ilhas de calor no município de Goiânia/GO (1986–2010). Boletim Goiano de Geografia 31: 113–127. https://doi.org/10.5216/bgg.v31i2.16849
20. O'Neill BC, Tebaldi C, van Vuuren DP, Eyring V, Friedlingstein P, Hurtt G, Knutti R, Kriegler E, Lamarque JF, Lowe J, Meehl GA, Moss R, Riahi K, Sanderson BM. 2016. The Scenario Model Intercomparison Project (ScenarioMIP) for CMIP6. Geoscientific Model Development 9: 3461–3482. https://doi.org/10.5194/gmd-9-3461-2016
21. O'Reilly CH, Brunner L, Qasmi S, Nogherotto R, Ballinger AP, Booth B, Befort DJ, Knutti R, Schurer AP, Ribes A, Weisheimer A, Coppola E, McSweeney C. 2024. Assessing observational constraints on future European climate in an out-of-sample framework. npj Climate and Atmospheric Science 7: 95. https://doi.org/10.1038/s41612-024-00648-8
22. Ortega G, Arias PA, Villegas JC, Marquet PA, Nobre P. 2021. Present-day and future climate over central and South America according to CMIP5/CMIP6 models. International Journal of Climatology 41: 6713–6735. https://doi.org/10.1002/joc.7221
23. Perkins-Kirkpatrick SE, Lewis SC. 2020. Increasing trends in regional heatwaves. Nature Communications 11: 3357. https://doi.org/10.1038/s41467-020-16970-7
24. Ramarao MVS, Arunachalam S, Sánchez BN, Schinasi LH, Bakhtsiyarava M, Caiaffa WT, Dronova I, O'Neill MS, Avila-Palencia I, Gouveia N, Ju Y, Kephart JL, Rodríguez DA. 2024. Projected changes in heatwaves over Central and South America using high-resolution regional climate simulations. Scientific Reports 14: 23145. https://doi.org/10.1038/s41598-024-73521-6
25. Requia WJ, Hoinaski L, Yang J, Adams MD, Yazdi MD, Rodrigues da Silva Júnior FM, Nascimento Saldiva PH, Koutrakis P. 2025. The role of green areas in modifying heat-related circulatory and respiratory hospital admissions in Brazil. Environment International 203: 109791. https://doi.org/10.1016/j.envint.2025.109791
26. Riahi K, van Vuuren DP, Kriegler E, Edmonds J, O'Neill BC, Fujimori S, Bauer N, Calvin K, Dellink R, Fricko O, Lutz W, Popp A, Cuaresma JC, KC S, Leimbach M, Jiang L, Kram T, Rao S, Emmerling J, Ebi K, Hasegawa T, Havlik P, Humpenöder F, Da Silva LA, Smith S, Stehfest E, Bosetti V, Eom J, Gernaat D,

Masui T, Rogelj J, Strefler J, Drouet L, Krey V, Luderer G, Harmsen M, Takahashi K, Baumstark L, Doelman JC, Kainuma M, Klimont Z, Marangoni G, Lotze-Campen H, Obersteiner M, Tabeau A, Tavoni M. 2017. The Shared Socioeconomic Pathways and their energy, land use, and greenhouse gas emissions implications: an overview. Global Environmental Change 42: 153–168. https://doi.org/10.1016/j.gloenvcha.2016.05.009

27. Sousa SB, Ferreira LG. 2012. Análise da temperatura de superfície em ambientes urbanos: um estudo por meio de sensoriamento remoto no município de Goiânia, Goiás (2002–2011). Confins 15. https://doi.org/10.4000/confins.7631
28. Souza EB, Ferreira DBS, da Cunha AC, de Souza FG, Braga RHM, Sousa AML, Gutierrez CBB, Carmo AMC, Costa LRR, Corrêa WPM, Dias TSS, Sodré VSF, Paca VHM, Bitencourt DP, Silva Junior JA, Souza-Filho PWM, Rocha GM, Ambrizzi T. 2026. Projected heatwave hazards in an eastern Amazonian metropolis under contrasting CMIP6 scenarios. Scientific Reports 16: 25499. https://doi.org/10.1038/s41598-026-57944-x
29. Thrasher B, Wang W, Michaelis A, Melton F, Lee T, Nemani R. 2022. NASA Global Daily Downscaled Projections, CMIP6. Scientific Data 9: 262. https://doi.org/10.1038/s41597-022-01393-4
30. Zhang X, Alexander L, Hegerl GC, Jones P, Klein Tank A, Peterson TC, Trewin B, Zwiers FW. 2011. Indices for monitoring changes in extremes based on daily temperature and precipitation data. Wiley Interdisciplinary Reviews: Climate Change 2: 851–870. https://doi.org/10.1002/wcc.147

Figures

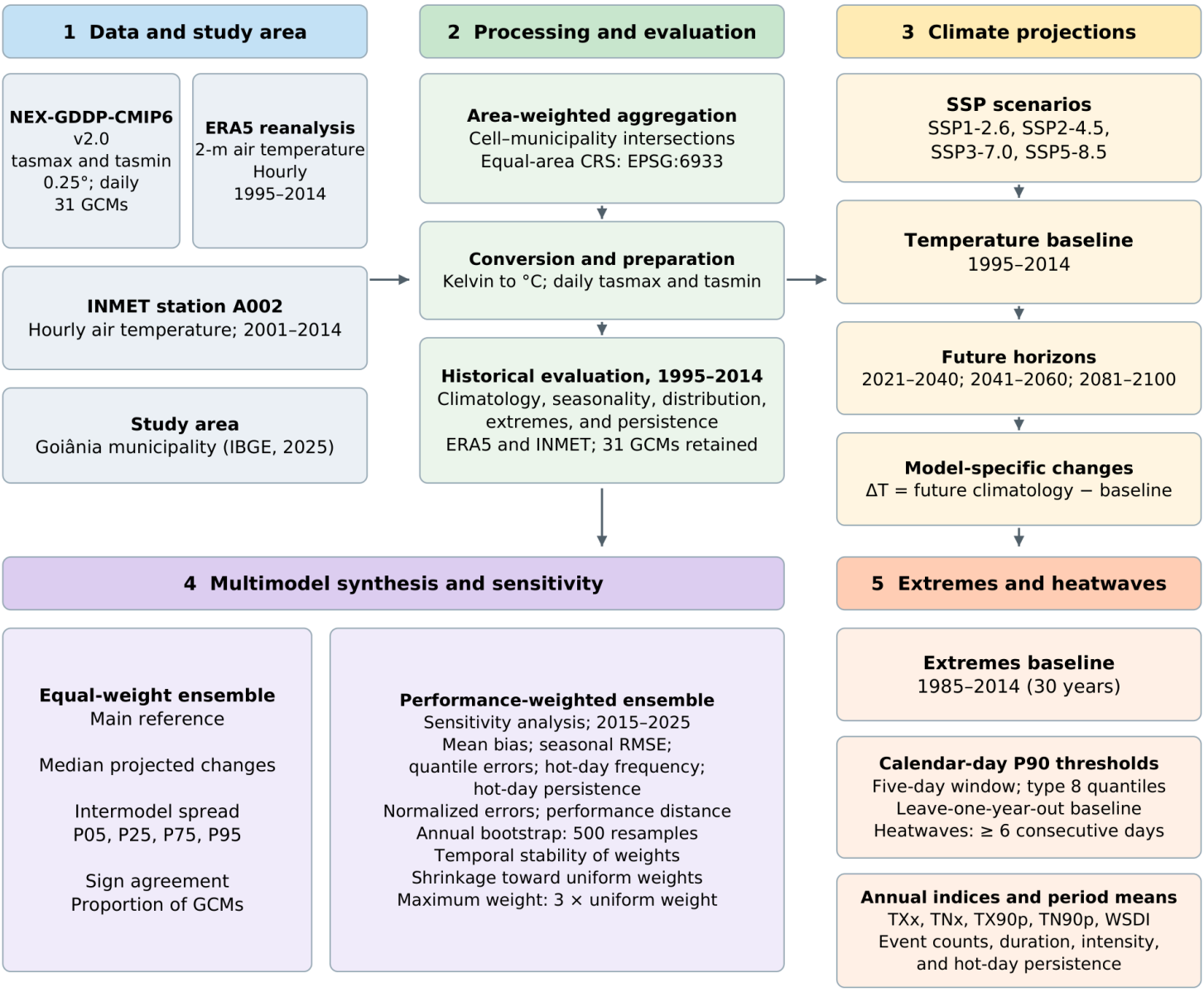


Figure 1

Methodological workflow for temperature and extreme-event projections.

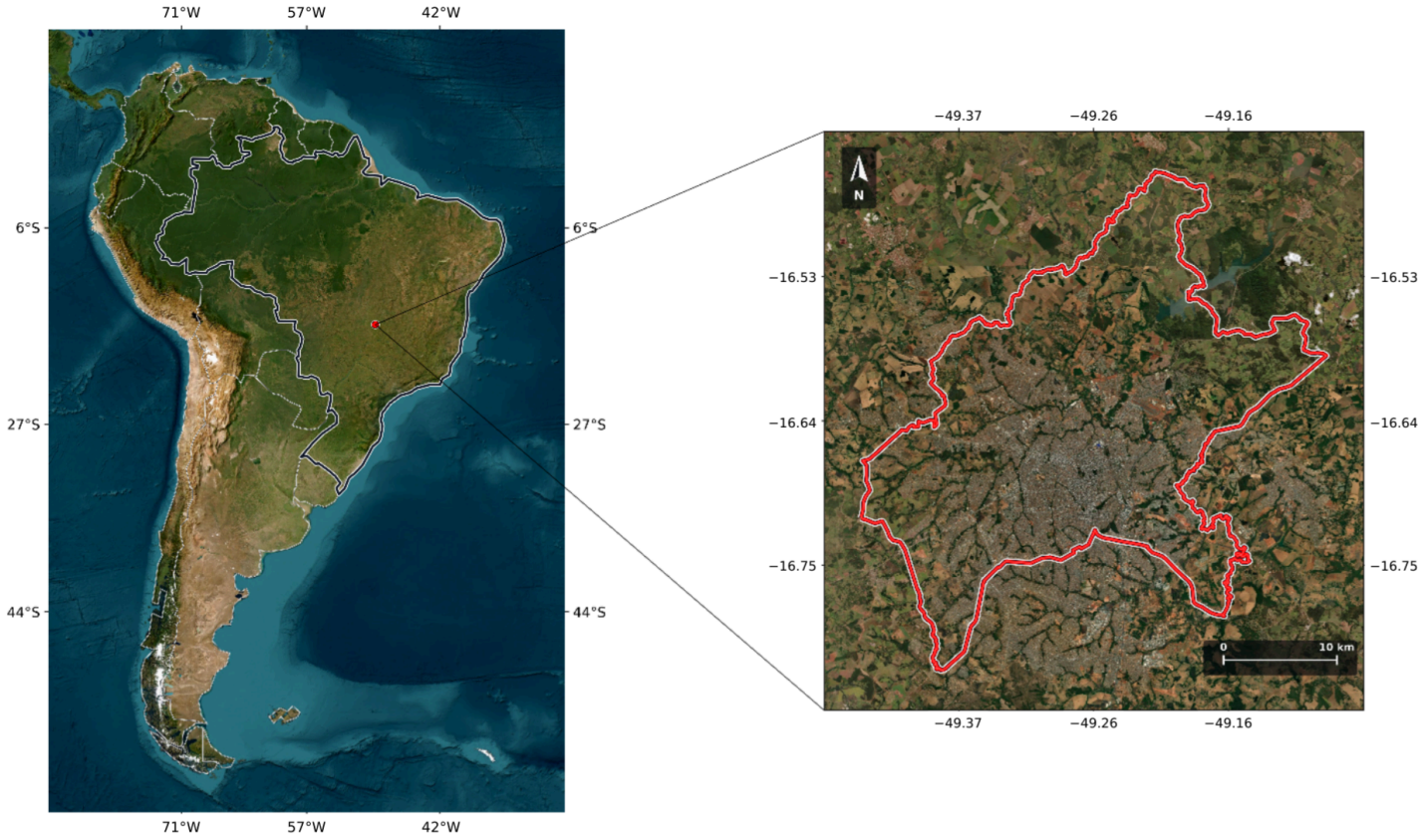


Figure 2

Location of Goiânia municipality, Goiás, Brazil.

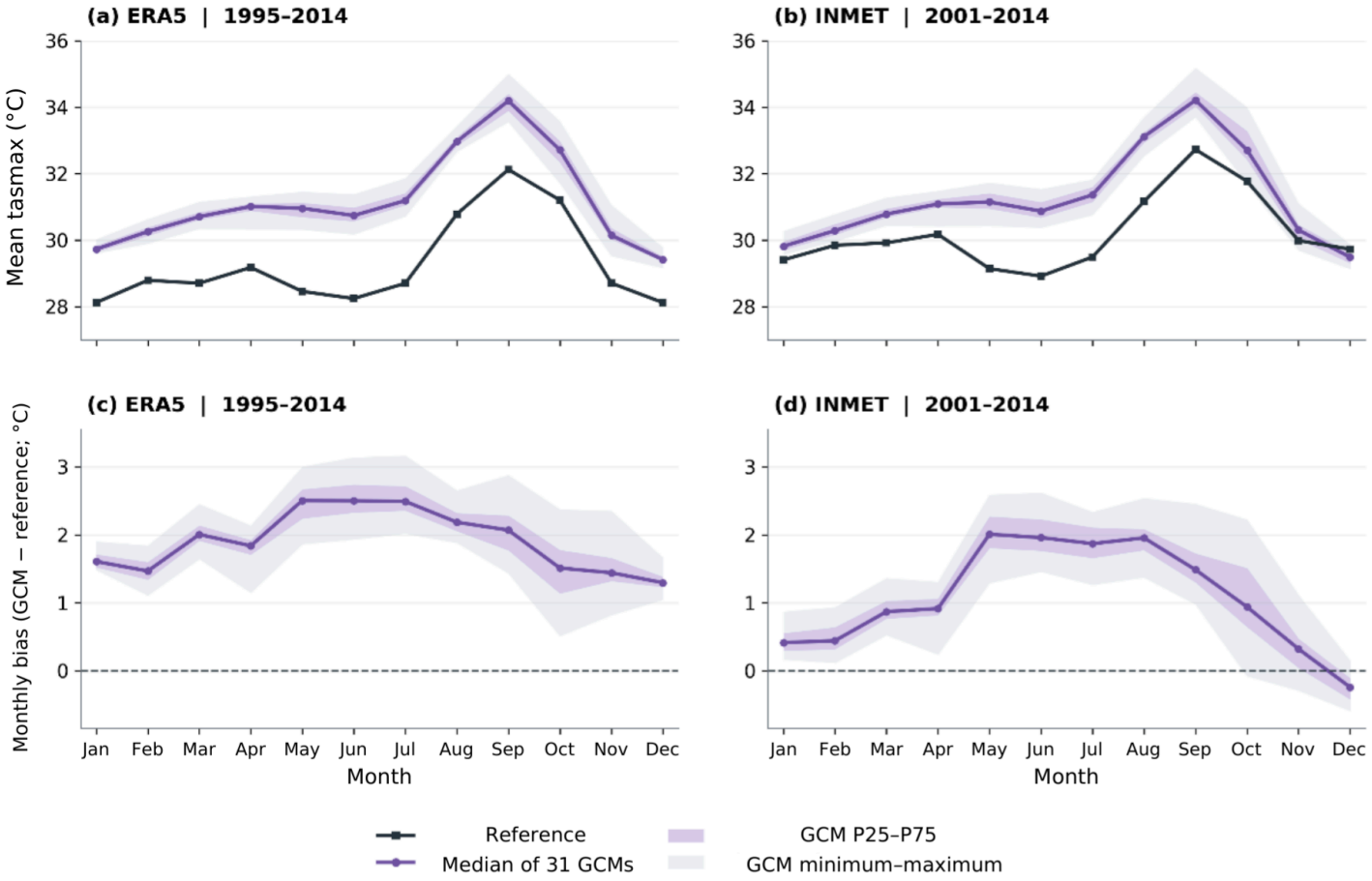


Figure 3

Monthly climatological cycles of maximum temperature for the 31 GCMs and the ERA5 (a) and INMET (b) references, with corresponding monthly biases (c–d).

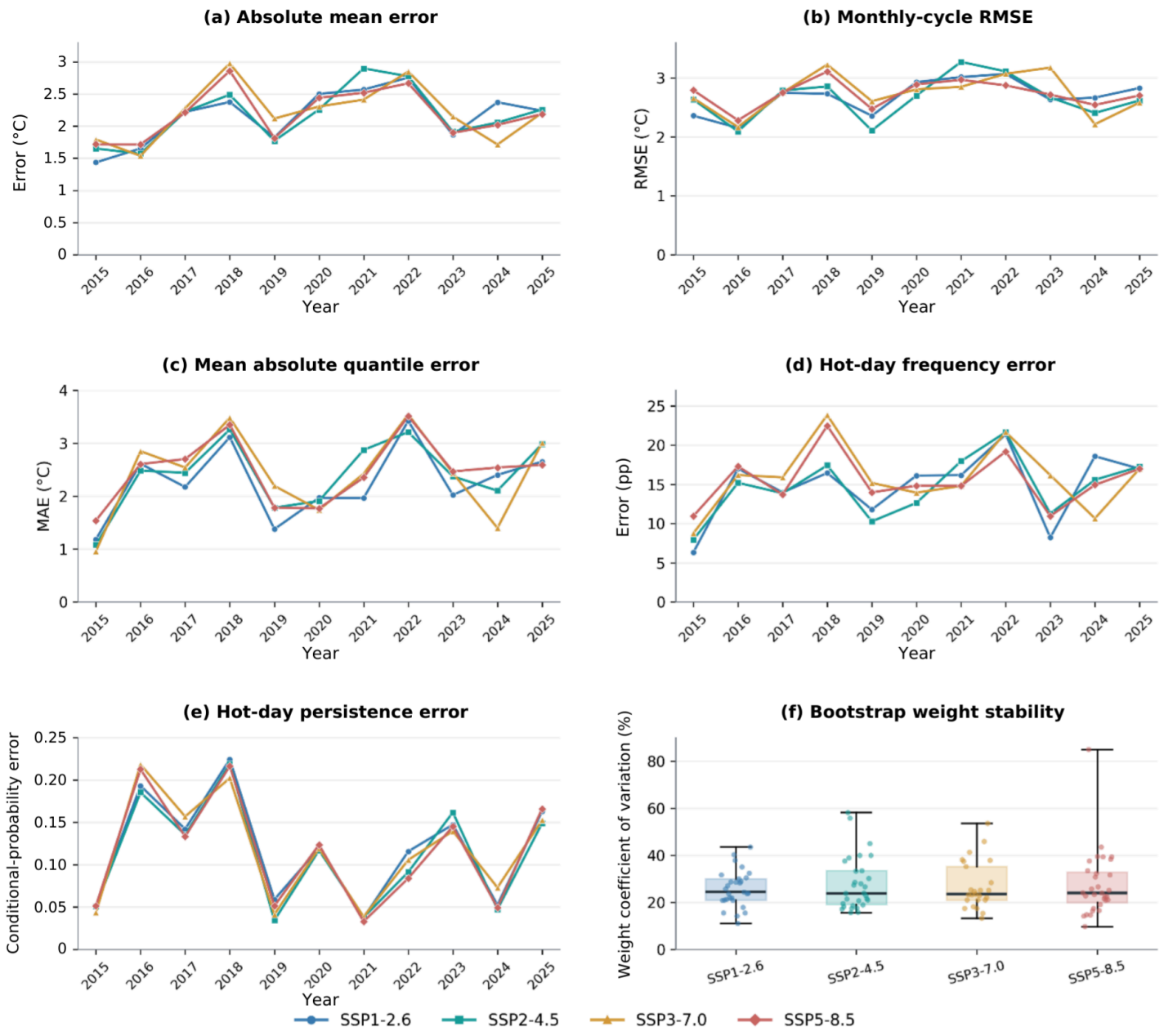


Figure 4

Annual intermodel medians of the five performance criteria against ERA5 during 2015–2025 (a–e), and distributions of weight coefficients of variation across 500 annual bootstrap resamples (f).

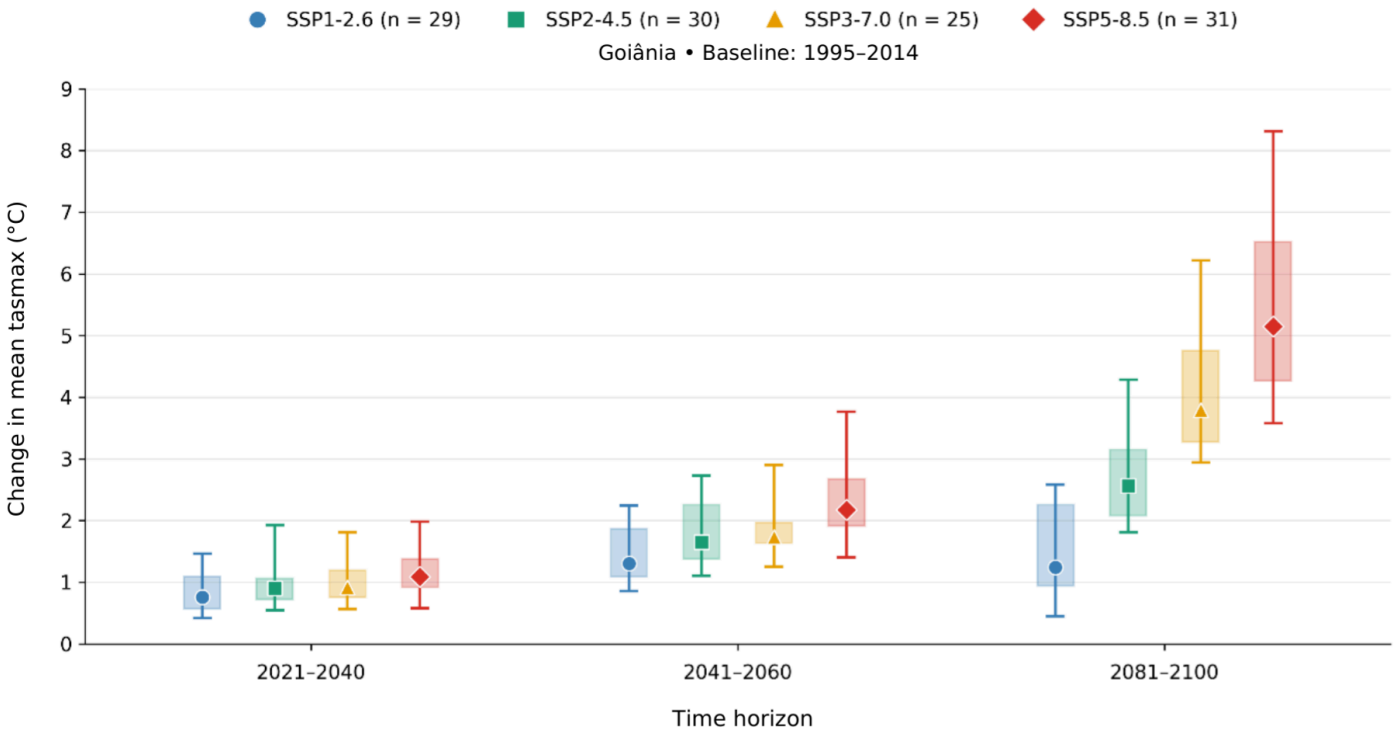


Figure 5

Projected changes in mean daily maximum temperature in Goiânia relative to 1995–2014.

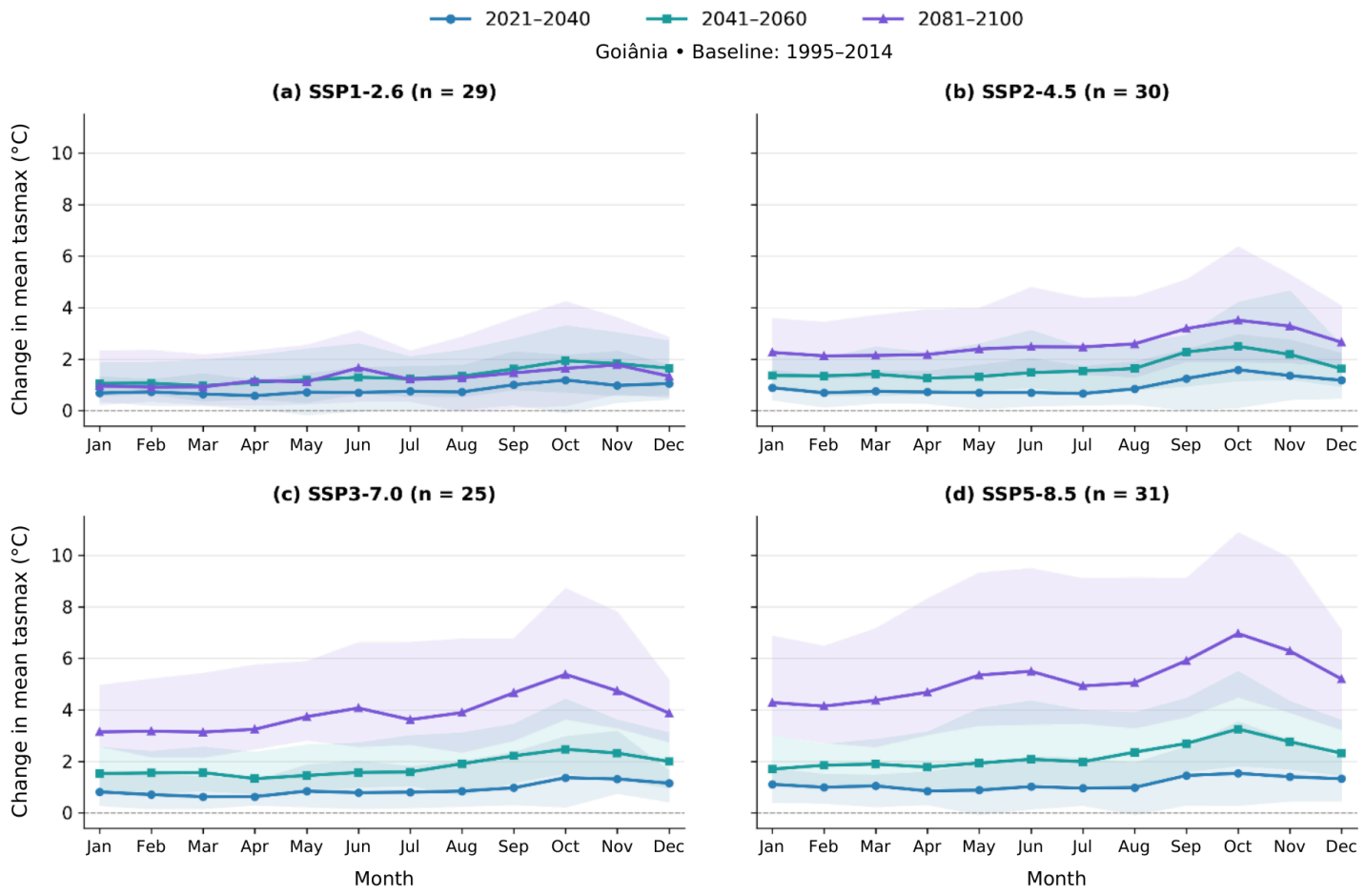


Figure 6

Monthly changes in mean daily maximum temperature in Goiânia relative to 1995–2014 under SSP1-2.6 (a), SSP2-4.5 (b), SSP3-7.0 (c), and SSP5-8.5 (d).

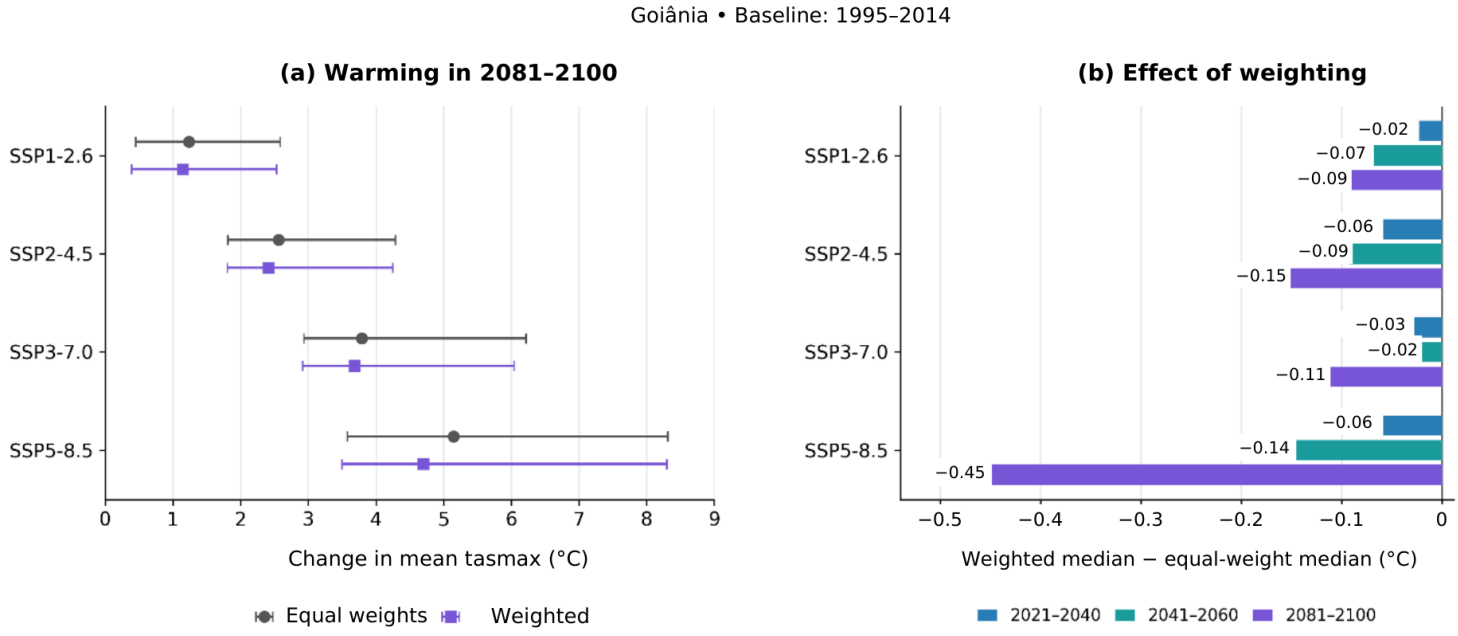


Figure 7

Sensitivity of projected mean daily maximum-temperature changes to model weighting. (a) Medians and P05–P95 intervals for the equal-weight and weighted ensembles in 2081–2100. (b) Differences between weighted and reference medians across the three time horizons.

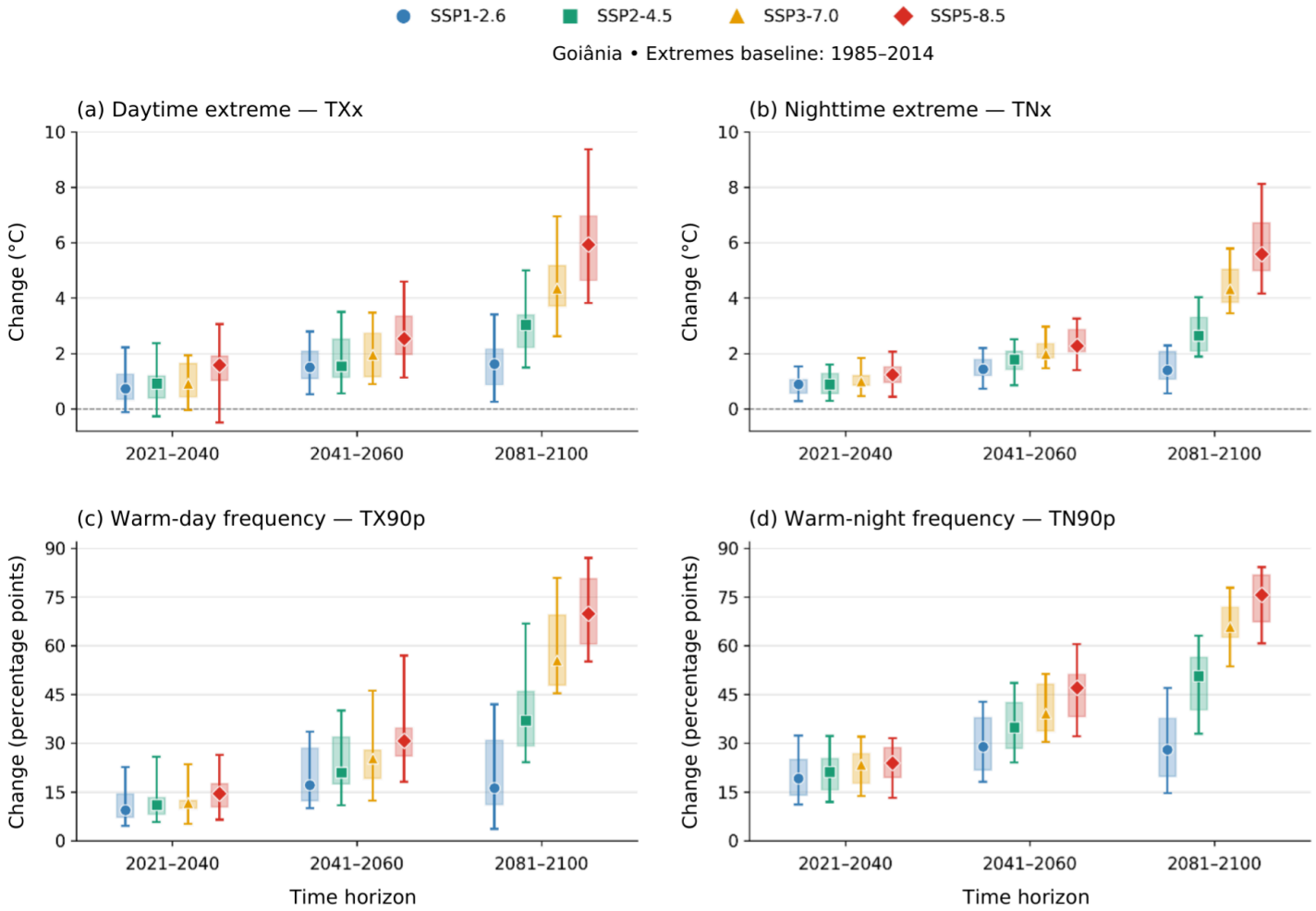


Figure 8

Projected changes in TXx (a), TNx (b), TX90p (c), and TN90p (d) in Goiânia relative to 1985–2014.

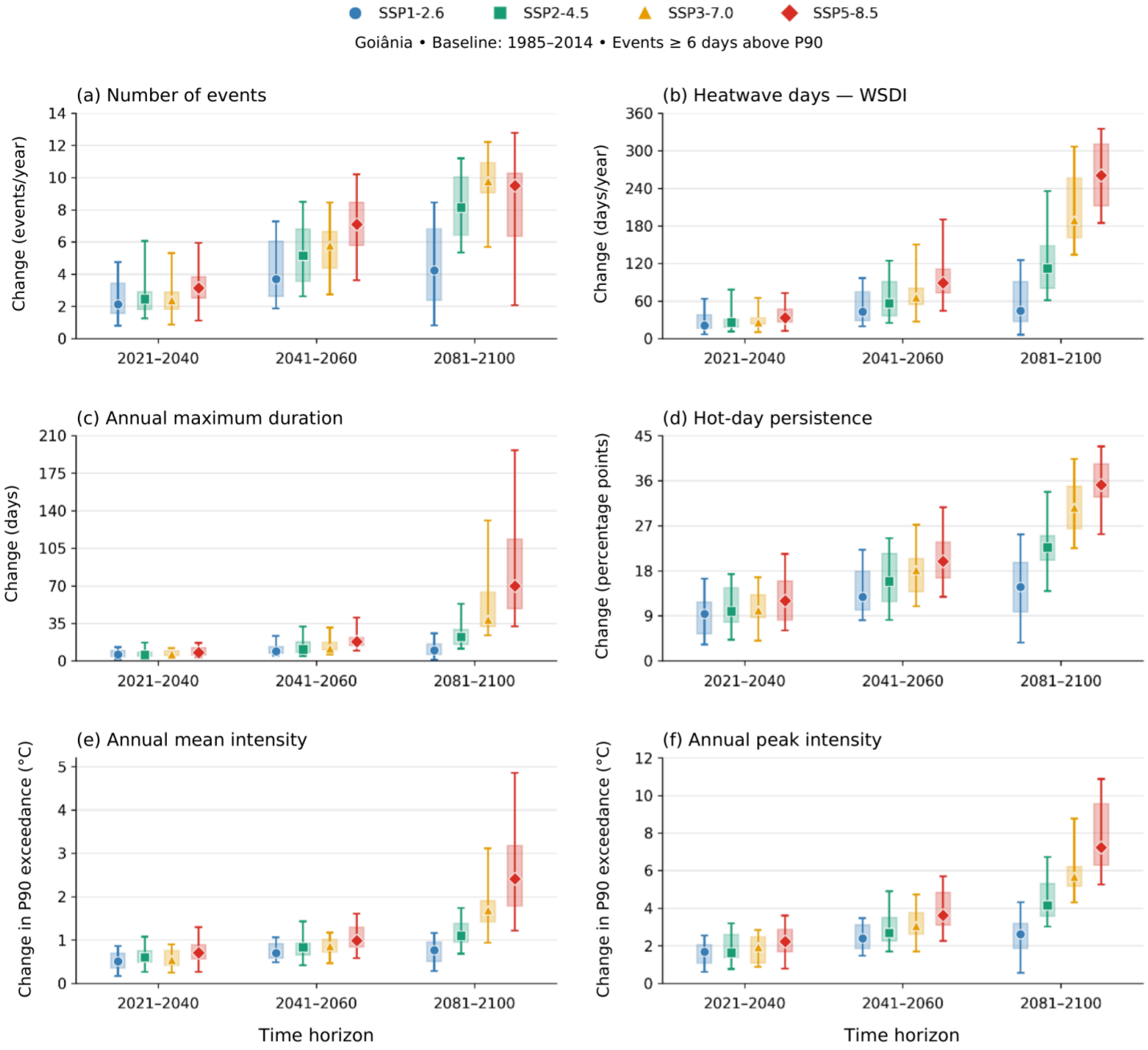


Figure 9

Projected changes in annual event counts (a), annual heatwave days (WSDI; b), annual maximum duration (c), hot-day persistence (d), annual mean intensity (e), and annual peak intensity (f), relative to 1985–2014.